[Article ID] 1003- 6326(2002)05- 0960- 06

Effect of different heat treatment process on damping peak of 6061Al/SiC_p MMC produced by spray codeposition①

GU Jin-hai(顾金海)[1], ZHANG Qing-xiao(张清霄)[2], GU Min(顾 敏)[1], WANG Xi-ke(王西科)[1], WANG Can(王 灿)[3], ZHU Zheng-gang(朱震刚)[3]

(1. Research Center for Materials, Zhengzhou University, Zhengzhou 450002, China;
2. College of Mechanical and Electronic Engineering, Zhengzhou University, Zhengzhou 450002, China;
3. Laboratory of Internal Friction and Defects in Solids, Institute of Solid State Physics, Hefei 230031, China)

[Abstract] Effects of five typical heat treatment processes on the damping properties and the damping peak of 6061Al/SiC_p MMC fabricated by spray codeposition were studied. The results show that the internal friction spectra of various heat treated samples exhibit the damping peak versus temperature between 130 ℃ and 200 ℃. Furthermore, the peak temperature as well as the peak height increases with increasing frequencies. By Arrhenius equation the active energy of the damping peak can be gotten, which is above 1 eV. On the other hand, different quenching treatments affect the damping peak remarkably, when the rate of cooling is above that of water quenching, the damping peak will shift to higher temperature as cooling speed is enhanced.

[Key words] spray codeposition; 6061Al/SiC_p MMC; heat treatment; damping capacity; damping peak

[CLC number] TG 113.226 **[Document code]** A

1 INTRODUCTION

Particulate-reinforced aluminum matrix composites have been currently investigated since they offer excellent damping capacity, in combination with high specific strength, stiffness and wear resistance[1~3]. Among the various synthesis methodologies which have been developed to fabricate MMCs, spray codeposition is viewed as the most promising technology for its potential of the minimization of deleterious interfacial reactions, the refinement of grain morphology, the increase in solid solubilities and the absence of macrosegregation[4, 5]. Aluminum alloys with high damping capacity have been applied broadly in the industry of aerospace, space and shipbuilding. By the internal friction measurements we can not only get the macro-information about damping capacity, but also explore the microstructure of material, the existing state and movement of deflects. Furthermore, each damping peak corresponds to a mechanical spectrum, these spectra will afford the basic data for the design and application of damping materials, whose mechanism will also offer theoretical guidance for the development of the new damping materials.

The damping behavior of 6061Al matrix MMCs reinforced by SiC particulate has been reported by Zhang, Perez and Lavernia[6, 7], but they didn't mention the damping peak versus temperature among the range of 130 ℃ and 200 ℃. In addition, Wang et al[8] and Zhang et al[9] have reported this damping peak, however, the samples in their studies were limited to T6 state (solutionizing at 530 ℃ for 1 h, quenching in water; aging at 175 ℃ for 8 h). For these reasons, emphases would be put on analyzing the damping peak occurred in the various heat treated samples produced by spray codeposition in the present study, and then, the damping mechanism involved were discussed.

2 EXPERIMENTAL

2.1 Preparation of samples and technology of heat treatment

Composite samples containing 14% SiC particulate(α phase volume fraction), were produced by spray codeposition. The metal matrix utilized in this study was 6061 Al alloy. The mean size of the SiC particles was about 10 μm. All of the spray atomized and deposited materials were then extruded at 400 ℃ using an area reduction ratio of 10:1 to close the micrometer sized pores that are normally associated with spray atomized and deposited materials. Samples for the internal friction measurements with dimensions of 3 mm × 1 mm × 70 mm were prepared by spark cutting.

Subsequently, all of the samples were grouped and numbered, and heat treatments were conducted accordingly for each group of samples. The systems of various heat treatments were specified as follows: 1) 530 ℃, 1 h solution heat treatment followed by being cooled in furnace and then aged(simplified as furnace cooled); 2) 530 ℃, 1 h solution heat treatment followed by being cooled in the air and then aged(simplified as air cooled); 3) 530 ℃, 1 h solution heat treatment followed by being quenched in water and then aged(simplified as water quenched); 4) 530 ℃,

① [Received date] 2001- 11- 26; [Accepted date] 2002- 02- 20

1 h solution heat treatment followed by being quenched in - 70 ℃ dry ice and then aged(simplified as - 70 ℃ quenched); 5) 530 ℃, 1 h solution heat treatment followed by being quenched in - 195 ℃ liquid state nitrogen and then aged (simplified as - 195 ℃ quenched). The aging process above mentioned refers to maintaining temperature at 175 ℃ for 8 h.

2.2 Testing of internal friction and analyses of TEM

Using a multifunctional internal friction instrument made by the Institute of Solid State Physics of the Academy of Science of China, the damping capacities of various heat treated samples were measured over temperature range from 20~ 400 ℃, not only for determining the relationship of internal friction (Q^{-1}) vs temperature(T) at frequencies of 0.1, 0.3, 1.0 and 3.0 Hz, but also for determining the relationship of internal friction(Q^{-1}) vs strain magnitude(ε) at a constant frequency of 1.0 Hz.

The analyses of microstructure of all the heat treated samples were carried out by Philips-CM200 type advanced TEM. TEM samples were thinned by the chemical method, and subsequently drilled.

3 RESULTS

The curves of internal friction(Q^{-1}) vs temperature(T) were plotted for air cooled sample and - 70 ℃ quenched sample in light of measured damping data, as shown in Fig. 1 and Fig. 2, respectively. After subtracting a background damping consisting of a superposition of a linear and an exponential term (as dot line shown in Figs. 1, 2), we can get the bare damping peaks vs temperature at frequencies of 0.1, 0.3, 1.0 and 3.0 Hz. The enlarged damping peaks of two aforementioned samples were shown in Fig. 3 and

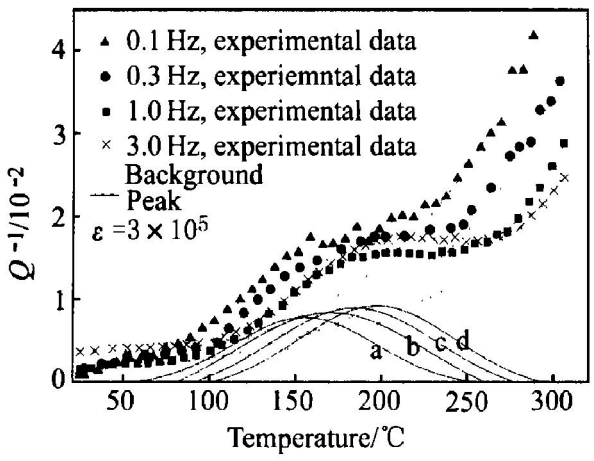

Fig. 1 Damping peaks versus temperature of air cooled sample obtained by subtraction of background damping(dot line) at different frequencies
(a) —0.1 Hz; (b) —0.3 Hz; (c) —1.0 Hz; (d) —3.0 Hz

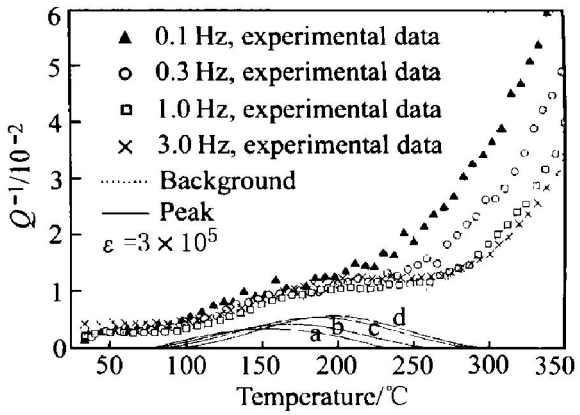

Fig. 2 Damping peaks versus temperature of - 70 ℃ quenching sample obtained by subtraction of background damping (dot line) at different frequencies
(a) —0.1 Hz; (b) —0.3 Hz; (c) —1.0 Hz; (d) —3.0 Hz

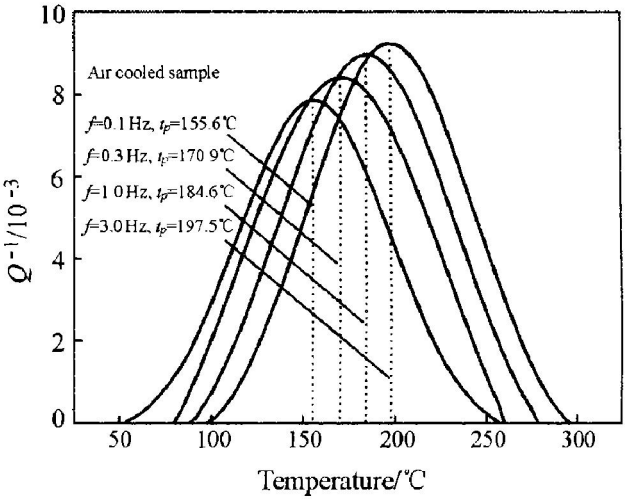

Fig. 3 Damping peaks versus temperature of air cooled sample

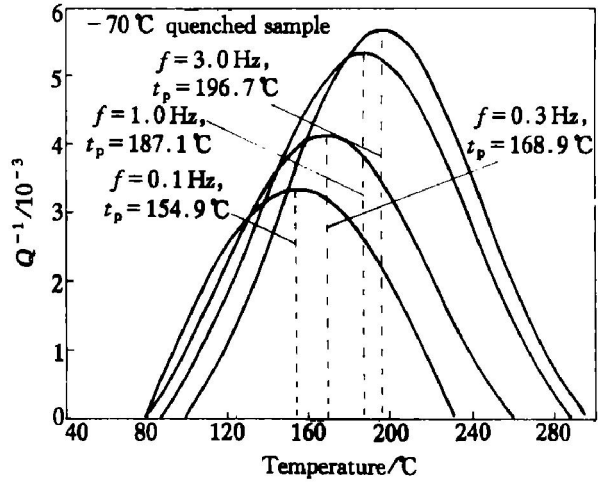

Fig. 4 Damping peaks versus temperature of - 70 ℃ quenching sample

Fig. 4. In fact the background damping herein is high temperature damping, which relates to the defects inside polycrystalline metals and alloys including dislocations and vacancies. The anelastic character of background damping attributes to broad relaxation

spectra, which arise from relaxation process in the control of diffusion, and it is compound results of several mechanisms[10].

According to the above mentioned method used to obtain damping peak, we dealed with the internal friction spectra of other heat treated samples. The results show that damping peaks always exist for case of all samples, and that the peak temperatures t_p appear at 130 ℃ to 200 ℃. More details about t_p are shown in Table 1. As is known to all, relaxation strength Δ can be calculated from the damping peak height Q_p^{-1}, and relaxation time τ can be obtained from peak temperatures. These are realized by using Arrhenius equation, which is expressed by[8, 10]

$$\tau = \tau_0 e^{H/kT} \quad (1)$$

where τ_0 is the inverse attempt frequency, H is the activation energy and k is Boltzmann's constant. At the peak temperatures t_p, the circle frequency ω is related to the relaxation time τ by $\omega\tau = 1$. Thereby, Eqn. (1) can be described by a new expression as

$$\lg\omega + \lg\tau_0 + (H/2303k)(1000/t_p) = 0 \quad (2)$$

In light of the data in Table 1, we obtained the Arrhenius plot shown in Fig. 5. Then the activation energy H and the inverse attempt frequency τ_0 were got as listed in Table 2. It can be seen that the activation energies of all the heat treated samples are above 1 eV, and the inverse attempt frequencies are between 10^{-15} and 10^{-21}.

In addition, the dependence of the internal friction on temperature for various strain amplitudes

Table 1 Variation of peak temperatures in different states of heat treatment with frequency

Sample	t_p / ℃			
	0.1 Hz	0.3 Hz	1.0 Hz	3.0 Hz
Furnace cooled sample	151.1	162.2	176.0	187.8
Air cooled sample	155.6	173.6	184.6	197.5
Water quenched sample	131.3	145.2	161.8	178.1
- 70 ℃ quenched sample	152.5	168.9	187.1	196.7
- 195 ℃ quenched sample	164.2	174.3	187.7	197.8

Table 2 Activation energy H and inverse attempt frequency τ_0 in different states of heat treatment

Sample	H / eV	τ_0
Furnace cooled sample	1.55	6.21×10^{-19}
Air cooled sample	1.42	3.85×10^{-17}
Water quenched sample	1.14	9.34×10^{-15}
- 70 ℃ quenched sample	1.36	1.68×10^{-16}
- 195 ℃ quenched sample	1.77	6.74×10^{-21}

($\varepsilon = 5, 10, 20, 40\times10^{-6}$) for water quenched sample, measured at a constant frequency of 1.0 Hz, is shown in Fig. 6. It can be seen that the dependence of damping on strain amplitude is not apparent in the whole measuring temperature range.

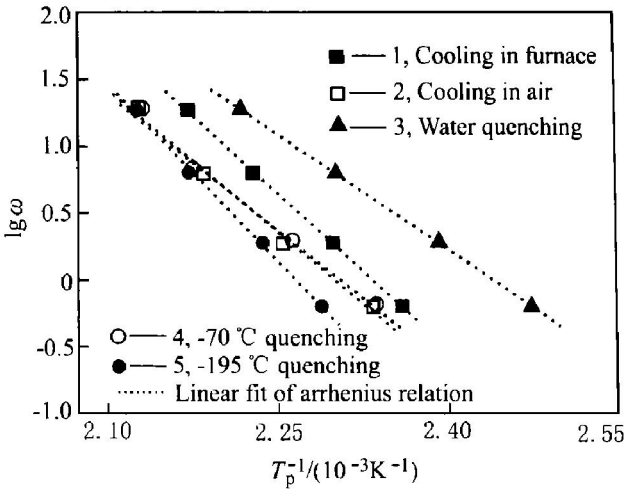

Fig. 5 Arrhenius relation between circle frequency and peak temperature deduced from data shown in Table 1

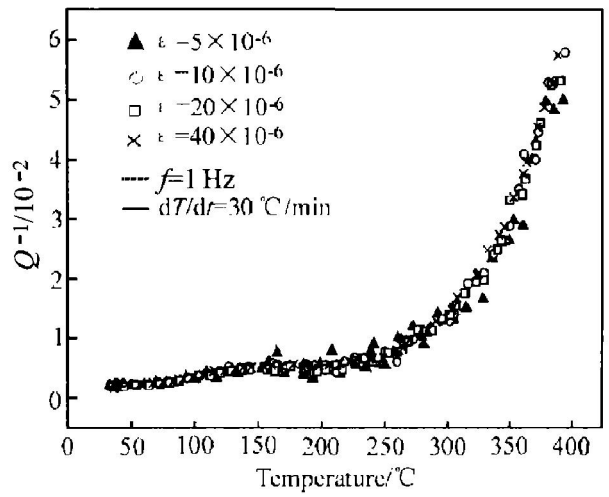

Fig. 6 Internal friction spectra of water quenched sample at various strain amplitudes

4 DISCUSSION

4.1 Analysis of damping mechanism

The characteristic of the curves of internal friction Q^{-1} vs temperature T, for all samples in different states of heat treatment, is that there exists temperature damping peaks between 130 ℃ and 200 ℃, whereas they don't exist in 6061Al[8, 9]. The absence of the damping peak in matrix alloy indicates that the modified microstructure of the matrix would be responsible for the appearance of the peak, and these modifications mainly owe to the introduction of particulate/matrix interfaces and thermal mismatch induced dislocation in the adjacent matrix.

Several studies[6~9] have shown that thermoelastic damping and grain boundary damping don't play a dominant role in the resultant damping of the MMC. The interface damping is resulted from the mobility of the incoherent microstructure at the interface and interface slip. Generally, there is a well bonded interface between the

SiC particulate and 6061Al matrix[11]. When the temperature is elevated above 100 ℃, the metal matrix may become soft relative to the ceramic particulate, and a movement at the interface is likely to occur. Therefore the interface damping may be dominant for 6061Al/SiC_p at elevated temperature. Accordingly, at high temperature, the high background damping of the MMC can be attributed to the interface damping.

On the other hand, The coefficient of thermal expansion (CTE) for SiC is 5(in units of 10^{-6} ℃$^{-1}$), whereas a value of 25 is generally reported for 6061Al[2, 8]. When the composite is cooled from elevated temperatures of annealing or processing, mismatch strains occur due to differential thermal contraction at the Al/SiC interface, which are sufficient to generate dislocations. The residual strain, or strain accumulation, produced as a result of the thermal mismatch, may be calculated from

$$\varepsilon = \Delta\alpha \times \Delta T \tag{3}$$

where ΔT is the temperature change and $\Delta\alpha$ is the difference between the CTEs of reinforcement and matrix. Because of the thermal mismatch strains, the plastic deformation will take place, and so does subsequent high density dislocation, especially in the region adjacent to the Al/SiC interface. For example, typical morphology of dislocations around the SiC particulate in water quenched sample is shown in Fig. 7. In view of the dislocation prismatic punching model, the density of dislocation ρ can be determined by[12]

$$\rho = \frac{B\varepsilon v_f}{bt(1 - v_f)} \tag{4}$$

where ε is the thermal mismatch strain given by Eqn. (3), v_f is the volume fraction of ceramic reinforcement(SiC), b the Burfers vector, t the smallest dimension of the reinforcement and B the geometric constant. Vogelsang et al investigated the generation and distribution of dislocation at the Al/SiC interface by using in situ TEM[13], these dislocations will become a possible source of high internal friction under cyclic loading. In conclusion, dislocation damping is the primary damping mechanism especially at low temperature in this study, and the damping peaks must be related to dislocation motion. As is now well known, the dislocation damping may be interpreted with Granato-Lucke theory, which assumes that dislocation moves with vibration, then breaks away in the snowslide-like mode from weak pinning points (such as some solute atoms, precipitations, vacancies, etc.), and then forms the dislocation loop around hard pinning points (such as network node of dislocation, the second phase, etc.), consequently causes relaxation of the applied stress and dissipation of the mechanical vibration energy. As is shown in Fig. 8, the dislocations are pinned by fine precipitation in − 70 ℃ quenched sample. However, in our case, because the strain amplitude doesn't attain the critical value(above 10^{-3} in Ref. [14]) corresponding to the break-away of pinned dislocation line, there isn't distinct strain-amplitude dependency. According to the vibration-string model, the internal friction independent of strain amplitude(δ) can be deduced and given by[15]

$$\delta = \Delta \frac{\omega\tau}{1 + \omega^2\tau^2} \quad (\omega \ll \omega_0) \tag{5}$$

$$\Delta = \frac{8Gb^2}{\pi^3 C}\alpha\Lambda l^2 \tag{6}$$

$$\tau = Bl^2/(\pi^2 C) \tag{7}$$

where G is the shear modulus, B is damping coefficient, C the strain of dislocation line, Λ the dislocation density and l the length of dislocation string. From Eqn. (5), the relaxation damping appears and the maximum occurs when $\omega\tau = 1$. Besides, the dislocation density as well as its effective length will affect damping capacity of materials remarkably.

4.2 Effect of heat treatment on damping temperature

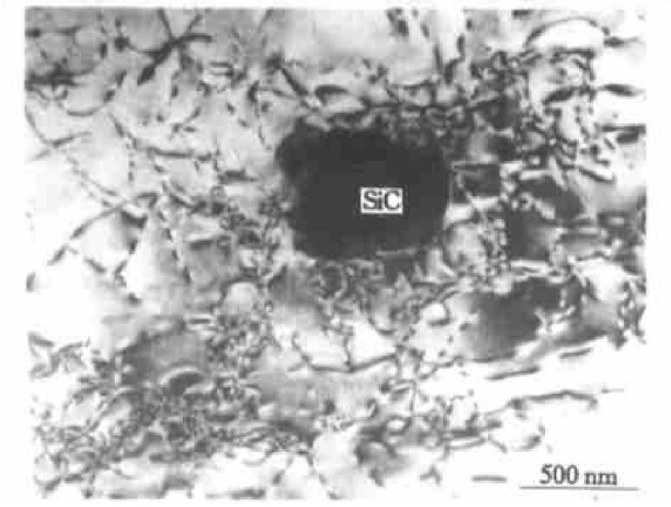

Fig. 7 Typical morphology of dislocations around SiC particulate (water quenched sample)

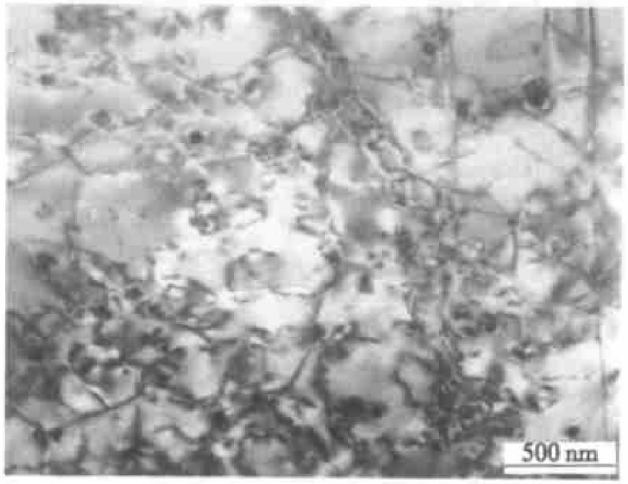

Fig. 8 Typical morphology of dislocations pinned by precipitation (− 70 ℃ quenched sample)

From Fig. 1 to Fig. 4, it is illustrated that the peak temperature increases with increasing frequencies, as well as the peak height. Furthermore, the relation of relaxation time and measuring temperature accords with Arrhenius equation. These phenomena are indicative of the relaxation characteristic of the damping peak, for which the reason is that the period of cyclic stress can be examined when it is comparative to relaxation time related to stress relaxation across the grain boundary. While frequency of vibration is enhanced, it needs higher temperature making relaxation time shorter and then the relaxation time is still as much as the period of vibration.

We compares the temperature damping peaks of the water quenched, - 70 ℃ quenched and - 195 ℃ quenched samples at a constant frequency of 1. 0 Hz.. The results are shown in Fig. 9 and Fig. 10. Obviously, with the quenching cooling rate increasing, the damping peak shifts to higher temperature. Due to the above-mentioned analysis, it can be proved as dislocation damping peak. According to Eqns. (3) and (4), the dislocation density resulting from thermal mismatch mechanism will increase remarkably with the increasing cooling rate of quenching. At the same time, concentration of the point defects will also increase. Consequently, the energies for climbing and dragging of dislocation will be enhanced, and the peak temperature will drift to higher temperature. This can be demonstrated from the data of active energies (shown in Table 2) of three heat treated samples, which shows itself as the increasing trend. In particular, the active energy(1. 77 eV) of - 195 ℃ quenched sample is by far higher than that(1. 45 eV) of self diffusion of aluminum[10], it shows that there must be the climbing mechanism involved in this sample.

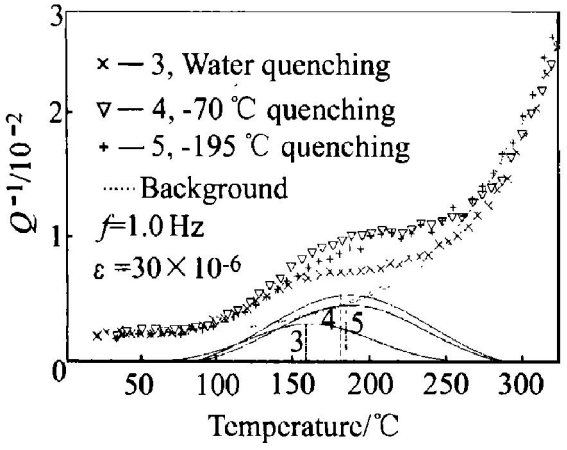

Fig. 9 Internal friction spectra and damping peak at constant frequency of 1. 0 Hz

5 CONCLUSIONS

1) When the strain amplitude ranges from 5 to 40 (in units of 10^{-6}), the dependence of damping on strain amplitude is not apparent in the whole temperature range.

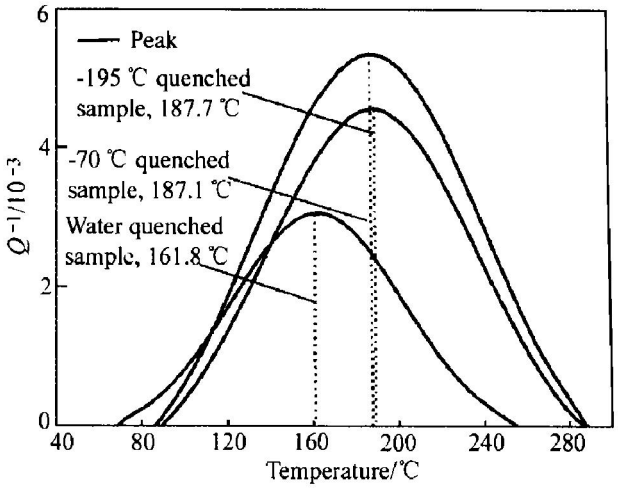

Fig. 10 Comparison of damping peaks at the same frequency

2) Damping peaks always appear over the range of 130 ℃ and 200 ℃ for five heat treated samples, the active energies calculated from Arrhenius equation are above 1 eV, and the inverse attempt frequencies are between 10^{-15} and 10^{-21}.

3) For all the heat treated samples, the peak temperature increases with increasing frequencies, and so does the peak height. These phenomena are indicative of the relaxation characteristic of the damping peak.

4) Different quenching treatment affects the damping peak remarkably. When the rate of cooling is above that of water quenching, the damping peak will shift to higher temperature as cooling speed is enhanced.

[REFERENCES]

[1] Ibrahim I A, Mohamed F A, Lavernia E J. Particulate reinforced metal matrix composites—a review [J]. J Mater Sci, 1991, 26: 1137- 1156.

[2] Zhang J, Perez R J, Lavernia E J. Documention of damping capacity of metallic, ceramic and metal-matrix composite materials[J]. J Mater Sci, 1993, 28: 2395- 2404.

[3] Severin I, Zgura G, Marinescu I. Microstructure evolution in 6063/SiC_p composites[J]. J Sci Eng Comp Mat, 1998, 7 (4): 315- 322.

[4] Wu Yue, Lavernia E J. Spray-atomized and codeposited 6061Al/SiC_p composites[J]. JOM, 1991, 43(8): 16- 23.

[5] Gupta M, Mohamed F A, Lavernia E J. The effect of ceramic reinforcements during spray atomization and codeposition of metal matrix composites[J]. Metall Trans A, 1992, 23A(3): 831- 843.

[6] Zhang J, Perez R J, Lavernia E J. Effect of SiC and graphite particulates on the damping behavior of metal matrix composites[J]. Acta Metall Mater, 1994, 42 (2): 395- 409.

[7] Lavernia E J, Perez R J, Zhang J. Damping behavior of

discontinously reinforced Al alloy metal matrix composites [J]. Metall Trans A, 1995, 26A: 2803– 2817.

[8] WANG Can, ZHU Zheng-gang. Internal friction at medium temperature in an Al matrix composite reinforced by SiC particles[J]. Scripta Mater, 1998, 38 (12): 1739– 1745.

[9] ZHANG Ying-yuan, LE Yong-kang, GAO Ling-qing. Damping characteristic and dislocation-induced damping mechanism of spray-atomized and codeposited 6061Al/SiC_p[J]. The Chinese Journal Nonferrous Metals, 1999, 9(1).

[10] GE Ting-sui. Theory Basis of Solid Damping. Relaxation and Structure of Grain Boundary, (in Chinese) [M]. Beijing: Science Press, 2000. 82– 83.

[11] Flom Y, Arsenault R J. Interfacial bond strength in an aluminum alloy 6061-SiC composite[J]. Mater Sci Eng, 1986, 77: 191– 197.

[12] Zhang J, Perez R J, Lavernia E J. Dislocation-induced damping in metal matrix composites[J]. J Mater Sci, 1993, 28: 835– 846.

[13] Vogelsang M, Arsenault R J, Fisher R M. An in situ HVEM study of dislocation generation at Al/SiC interfaces in metal matrix composites[J]. Matall Trans A, 1986, (17A): 379– 389.

[14] Hartman J T Jr, Keene K H, Arstrong R J, et al. Dislocation density determinations in composites[J]. JOM, 1986, 38 (4): 33– 35.

[15] FENG Duan. The Third Volume of Metal Physics. Mechanical Property of Metal, (in Chinese)[M]. Beijing: Science Press, 1999. 128– 130.

(Edited by LONG Huai-zhong)